A Deep-Sea Differential Pressure Gauge

CHARLES COX, THOMAS DEATON AND SPAHR WEBB

Scripps Institution of Oceanography, La Jolla, CA 92093

(Manuscript received 17 March 1984, in final form 2 July 1984)

ABSTRACT

A pressure gauge configured to respond to the difference between the ocean pressure and the pressure within a confined volume of compressible oil is found to be especially useful for detecting pressure fluctuations in the frequency range from a few millihertz to a few hertz. In the middle of the range its noise level is lower than any other known gauge. The limitation of the gauge at the lower frequency limit is caused by unpredictable thermal expansion in the confined oil and at the upper limit by thermal agitation noise in the resistance of the strain gauge transducer. The gauge is insensitive to acceleration and tilting. Measurements with this gauge on the deep seafloor show two principal features in the spectrum of pressure fluctuations. At frequencies below 0.03 Hz there is evidence of pressures generated directly by long surface gravity waves. Above 0.11 Hz the pressures associated with microseisms are predominant. Between 0.03 and 0.11 Hz there is a spectral gap where the pressure level drops below 0.1 Pa^2 Hz^{-1}.

1. Introduction

The spectrum of pressure fluctuations at the seafloor ranges from the very low frequencies associated with geologic changes in the ocean depths to very high-frequency sound waves. The device described here is most effective for detecting pressure oscillations in a small part of this range: three decades centered at 0.1 Hz. This range encompasses pressures generated by long ocean surface gravity waves, seismic disturbances of the seabed, microseisms, and the low-frequency end of the ocean acoustic spectrum (Fig. 1). The gauge is designed to be emplaced on the seafloor for relatively long periods with data recorded *in situ*.

The requirements that must be satisfied by such a recording pressure gauge are the following:

1) It should have adequate sensitivity and such low noise that it can detect the pressure signals in the band of interest. The pressure background spectrum is lowest between 0.03 and 0.10 Hz and falls at the upper limit of this band to values close to 10^{-2} Pa^2 Hz^{-1}.

2) It must be stable in the high ambient pressure of the seafloor and in the presence of the temperature fluctuations and accelerations to which it will be exposed.

3) It must withstand the stresses of transportation on shipboard, and to and from the seabed.

4) The electrical power required to operate the gauge must be moderate so that a battery supply can be used.

In addition, a useful gauge should be inexpensive and simple.

Various techniques have been used to measure pressures at the seabed. Quasi-absolute pressure measurements have been made with diaphragm gauges in which sensing of the motion of the diaphragm is carried out by vibrating strings, capacitive detectors, or vibrating quartz crystals. Filloux (1980) provided a review of some of these devices and described a bourdon tube element for detection of changes in absolute pressure. Absolute instruments are suitable for detection of tides and other low-frequency phenomena. In contrast, hydrophones are particularly effective at frequencies above a hertz, although Nichols (1981) reported background noise measurements extending below 0.1 Hz.

2. A differential method

Both absolute gauges and hydrophones appear to have severe noise problems in the frequency range of a hundredth to a few hertz. For the absolute gauges the problem resides in the enormous dynamic range required, while for hydrophones the limitation consists of thermal and "1/f" noise in the amplifiers. In our search for a simple technique we settled upon a scheme that measures the difference of pressure between the ocean and a reference. The latter is maintained by a compressible fluid that fills a rigid chamber (Fig. 2). By using a truly differential sensor we have avoided the problem of detecting minute pressure changes in the presence of the overall ocean pressure. For example, in the frequency band including the microseismic peak, the rms pressure excursions are a few pascals (1 Pa $\sim$ 0.1 mm of water pressure), whereas the seafloor pressure is typically 4×10^7 Pa.

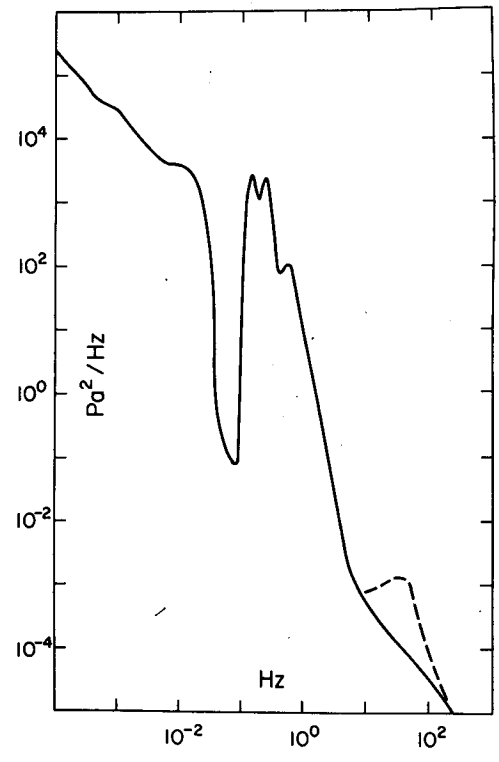

FIG. 1. Schematic spectrum of pressure on the deep seafloor. Data for the diagram were taken from the three sources: below 0.01 Hz from Filloux (1983; NE Pacific), between 0.01 and 10 Hz from the July 1983 observations reported here (NE Pacific), above 10 Hz from Perrone (1969; NW Atlantic). The dashed line shows the increase of intensity caused by ship noise in a heavily trafficked ocean area.

A modern form of differential pressure transducer which we find to be capable of withstanding the very high ambient pressure uses, as a sensing transducer, a thin diaphragm made of single crystal silicon on which a resistance stain gauge has been created and isolated from the bulk silicon by pn junctions. The diaphragm is exposed to sea pressure (through an insulating fluid) on one side and to the reference pressure on the other. A remarkable feature of the construction is that there are no bubbles or other hollow closed spaces which can be collapsed by the ambient sea pressure. Therefore, the transducer is inherently unaffected by the common mode pressure and need not be protected by a pressure case.

3. Relation of noise level to excitation power

The open circuit output voltage of a differential pressure, strain transducer follows the form

$$v = \lambda E \Delta p / p_0, \qquad (1)$$

where Δp is the pressure difference, p_0 the full-scale rating, E the excitation voltage for the bridge and λ a constant, approximately 0.014 for devices supplied by two manufacturers (Foxboro and I.C. Sensors, undated, Catalogue items 1800-04-01-008 and 20B-05-PSJD respectively, San Jose and Sunnyvale, CA.)

The noise level of a pressure measurement is comprised of two parts: interference from competing physical processes (acceleration, temperature, aging, etc.) that affect the signal and electrical noise. In a strain gauge transducer the latter consists of thermal agitation in the resistances of the gauge plus excess noise caused by electrical current flowing in the resistors. Noise may also be generated in the process of amplification of the signal. In our work we have minimized excess noise and amplifier noise by exciting the bridge with an alternating current, and demodulating the signal only after amplification. This process removes the effects of 1/f noise, which is the principal component of excess noise both in the bridge and in the amplifier.

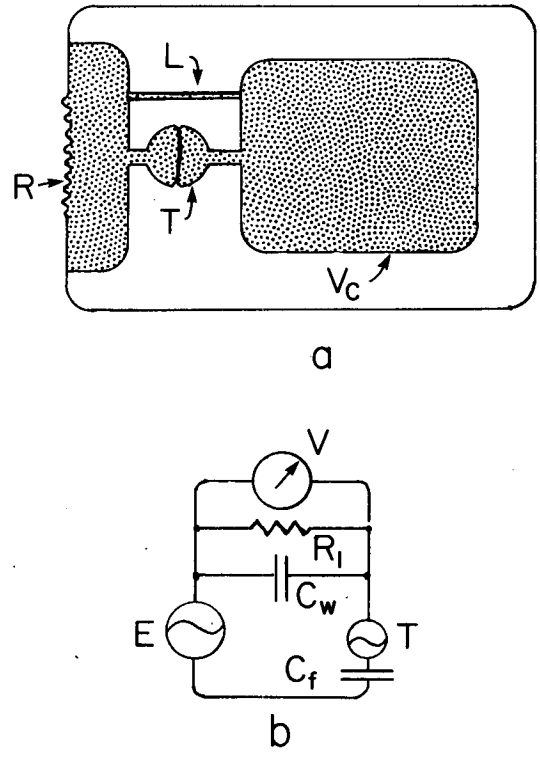

FIG. 2. (a) A differential pressure gauge. T is the strain gauge transducer which responds to the difference of pressure between the ocean and the fluid contained in the reference chamber V_c. The compressible fluid is shown stippled. The reference pressure is slowly relaxed to the ocean pressure by fluid flow through the capillary leak L. The ocean pressure is admitted through the flexible rubber diaphragm R. (b) The electrical circuit with response equivalent to the gauge shown in (a). E is a voltage source analogous to the ocean pressure and V is the analog of the differential pressure sensed by the strain transducer. Capacitances C_w and C_f represent the compliance of the reference chamber wall and of the fluid contained in it, respectively. R is the resistance of the capillary leak and T is the spurious signal introduced by thermal expansion of the fluid or the reference chamber.

The spectrum of electrical voltage caused by ocean pressure fluctuations with spectrum Sp is

$$\lambda^2 E^2 |X|^2 p_0^{-2} Sp, \tag{2}$$

where X is the transfer function relating measured pressure to the ocean pressure [see Eq. (16)]. The noise spectrum is

$$4kTR_1F_1,$$

where $4kTR_1$ represents the thermal noise voltage spectrum in the bridge output resistance R_1, and F_1 is a factor allowing for excess noise and amplifier noise. The signal to noise ratio is

$$SNRd = \frac{\lambda^2 W |X|^2 p_0^{-2} Sp}{4kTF_1}, \tag{3}$$

where $W = E^2/R_1$ is the excitation power (assuming equal resistances in all legs of the bridge). The manufacturer's rating is $W = 10$ mW; in our seafloor gauges we have operated with $W = 3.2$ mW to save power. According to our laboratory calibration the transfer function remains unity to frequencies below 0.01 Hz and the noise factor F_1 is less than 2. These quantities and the rated sensitivity of a 5 psi unit ($p_0 = 34\,000$ Pa, $\lambda = 0.014$) provide a minimum sensitivity as shown in Table 1.

The theoretical performance of a broadband ceramic hydrophone can be compared with these figures. At very low frequencies the impedance is capacitive. The signal is amplified with a direct coupled amplifier with the circuit shown schematically in Fig. 3. The resistance R_2 consists of the leakage resistance of the transducer in parallel with the input resistance of the amplifier. The signal voltage is $E = \gamma p$ and is applied in series with the capacitance of the transducer. At the input to the amplifier then, the signal voltage spectrum is

$$Sv = \frac{(\gamma\omega\tau)^2 Sp}{1 + \omega^2\tau^2}, \tag{4}$$

while the thermal noise spectrum is generated by the real part of the source impedance

$$Z = R_2(1 - j\omega\tau)/(1 + \omega^2\tau^2).$$

In these expressions $\tau = R_2C$ is the time constant of the input circuit. The signal to noise ratio is therefore

$$SNRc = \frac{(\gamma\omega\tau)^2 Sp}{4kTR_2F_2}, \tag{5}$$

TABLE 1. Sensitivity of pressure gauge.

W (mW)	E (volts)	R_1 (ohms)	Sp (at $SNRd = 1$) ($Pa^2\ Hz^{-1}$)	f* (Hz)
10	7	4700	1.9×10^{-5}	150
3.2	4	4700	6.1×10^{-5}	50

* Frequency at which the oceanic background spectrum shown in Fig. 1 drops to the level Sp of the preceding column.

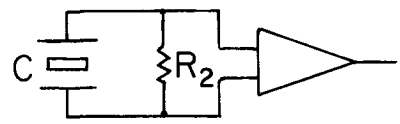

FIG. 3. The circuit of a ceramic hydrophone.

where F_2 is a factor allowing for amplifier or other excess noise. By comparison of Eqs. (3) and (5), we see that the pressure gauge has a better signal to noise ratio at low frequencies while the hydrophone is better at high frequencies. The crossover frequency occurs at

$$\omega_c = \frac{\lambda|X|}{\gamma p_0 C}\left(\frac{WF_2}{R_2F_1}\right)^{1/2}. \tag{6}$$

For a particular barium titanate transducer capable of working at the seafloor and of a size and mass comparable to the pressure gauge described here, the following parameters are appropriate:

$$\gamma = 10^{-4}\ \text{V Pa}^{-1},$$
$$C = 0.013\ \mu\text{F}$$

The crossover frequency in comparison with the silicon diaphragm pressure transducer ($\lambda = 0.014$, $p_0 = 34\,000$ Pa, $W = 10$ mW) depends on input resistance R_2 as follows:

R_1 (ohms)	$\omega_c/2\pi$ (hertz)
10^6	$5.0\lvert X\rvert\left(\frac{F_2}{F_1}\right)^{1/2}$,
10^8	$0.50\lvert X\rvert\left(\frac{F_2}{F_1}\right)^{1/2}$.

It is probably impractical to operate with input resistance much higher than 10^8 ohms because the leakage resistance of the ceramic transducer alone is measured at 10^{10} ohms and is rather unstable. Furthermore, it is doubtful that excess noise can be well controlled with such high values. For frequencies above 0.1 Hz, the factor $|X|(F_2/F_1)^{1/2}$ may be taken to be roughly unity. Therefore, a single silicon diaphragm pressure transducer is superior to certain ceramic hydrophones at frequencies below ~1 Hz. The advantage of the silicon devices can be extended into higher frequencies, at the expense of higher power by operating multiple units in parallel.

With respect to absolute pressure transducers, the comparison is not so clear, but the simplicity of achieving the required dynamic range by use of the differential arrangement is a strong recommendation for its use above about 0.01 Hz. For example, Filloux (1980, his Fig. 6) suggested that his deep sea observations were contaminated by 1/f noise at higher frequencies.

4. Response of a differential pressure gauge

We refer to Fig. 2a. The reference chamber with volume

$$V_c = V_c(p_a, p_f, T_c) \tag{7}$$

is filled with a compressible fluid with density

$$\rho_f = \rho_f(p_f, T_f). \tag{8}$$

Here p and T refer to pressure and temperature while subscripts f, a and c refer to the reference fluid, the external ambient and the reference chamber, respectively. The mass of fluid contained in the chamber is

$$m = \rho_f V_c, \tag{9}$$

whence its rate of change due to flow through the capillary leak is

$$\dot{m} = \dot{\rho}_f V_c + \rho_f \dot{V}_c. \tag{10}$$

The first time-varying term on the right can be represented [Eq. (8)] as

$$\dot{\rho}_f = (\partial\rho_f/\partial p_f)\dot{p}_f + (\partial\rho_f/\partial T_f)\dot{T}_{\text{cond}}. \tag{11}$$

Here we split up the temperature change into an adiabatic term driven by the pressure changes and (second term on the right) a term due to conductive heat flow through the chamber walls and driven by external heating and cooling. In reality, the pressure-induced temperature changes will also be affected by heat flow, but this can be neglected because only a thin boundary layer will be nonadiabatic. In terms of the adiabatic compressibility

$$k_f = \rho_f^{-1}(\partial\rho_f/\partial p)_{\text{adiabatic}}$$

and thermal expansion coefficient α_f, we write Eq. (11) in the form

$$\dot{\rho}_f = \rho_f(k_f\dot{p}_f - \alpha_f\dot{T}_{\text{cond}}). \tag{12}$$

In a similar way we write

$$\dot{V}_c = V_c(-k_1\dot{p}_a + k_2\dot{p}_f + \alpha_c T_c). \tag{13}$$

In this expression k_1 and k_2 allow for three processes: 1) The bulk compressibility of the chamber as a whole is

$$k_1 - k_2 = -V_c^{-1}\partial V_c/\partial p_a,$$

when $p_a = p_f$. 2) The elastic response of the chamber caused by differential pressure across the chamber wall is

$$-k_1\delta p_a + k_2\delta p_f = -\delta(p_a + p_f)k_b + \delta(p_f - p_a)k_d$$
$$= \text{bulk term} + \text{differential term},$$

where

$$k_b = k_1 - k_2 \quad \text{and} \quad k_d = (k_1 + k_2)/2.$$

Finally, (3) the compliance of the transducer and of the gaskets that seal the chamber is included in the term k_d.

Within the capillary leak, a thin cylindrical tube, the inward mass flux follows Poiseuille's expression provided the cylinder's length L is much greater than a typical cross-sectional scale r. The expression is

$$\dot{m} = Q\rho_f r^4(p_a - p_f)/(\eta L), \tag{14}$$

where Q is a constant (equal to $\pi/8$ if the cylinder is circular with radius r), and η is the viscosity of the fluid.

Suppose all pressure terms vary as $\exp(j\omega t)$ and that heat conduction is negligible. By combining (10)–(14) we find that

$$p_f = p_a \frac{1 + (j\omega\eta V_c L k_1)/Qr^4}{1 + (j\omega\eta V_c L(k_f + k_2)/Qr^4}. \tag{15}$$

The pressure transducer responds to the difference $p_a - p_f$. The transfer function $X = (p_a - p_f)/p_a$ is

$$X(\omega) = \frac{\omega\tau_2}{\omega(\tau_1 + \tau_2) - j}, \tag{16}$$

where

$$\tau_1 = \eta V_c L k_1/(Qr^4),$$
$$\tau_2 = \eta V_c L(k_f - k_b)/(Qr^4),$$
$$k_b = k_1 - k_2.$$

The electrical analog of this system is shown in Fig. 2b. The characteristic times are $\tau_1 = RC_w$, $\tau_2 = RC_f$ where C_w and C_f are the analogs of the compliance of the chamber wall and fluid, respectively. It will be noticed that deflections of the reference chamber wall reduce the high-frequency response of the system by a factor

$$\frac{\tau_2}{\tau_1 + \tau_2} = \frac{k_f - k_b}{k_f - k_2},$$

as compared to the response of an unyielding system. Therefore, the compliance of the chamber wall and of the transducer itself must be minimized in comparison with that of the fluid that fills the chamber.

5. Effect of temperature fluctuations

Suppose that the ambient pressure remains constant but that the temperature of the chamber and of its contents both vary according to $\exp(j\omega t)$. From Eqs. (10)–(13) one finds that the complex relation between temperature amplitudes and the amplitude of the reference pressure is

$$p_f = \frac{\alpha_f T_f - \alpha_c T_c}{k_f + k_2}\left[1 - \frac{j}{\omega(\tau_1 + \tau_2)}\right]. \tag{17}$$

This expression is a gross simplification of the actual situation in which temperatures, far from being uniform in the chamber wall and fluid fill, respectively, will vary only within thin boundary layers that lie closest to the sources of heat. Nevertheless, Eq. (17)

illustrates that the reference chamber must be thoroughly insulated from rapid changes of temperature. Representative values of the material properties are $\alpha_c = 7.5 \times 10^{-5}$ K^{-1} for the thermal expansion coefficient of aluminum and $k_f + k_2 = 0.8 \times 10^{-9}$ Pa^{-1}. Therefore, the temperature of the reference chamber must be kept constant to 11 μdeg to avoid errors as much as 1 Pa. The problem is easily solved for the frequency pass band of interest by placing thermal insulation around the pressure gauge (Fig. 4). The insulation consists of an oil-filled acrylic plastic jacket completely surrounding the reference chamber. By fastening the chamber to a single point of the jacket, the chamber is also shielded from stresses whether induced thermally or mechanically in the jacket. The sea pressure is admitted to the interior of the jacket through a flexible rubber band which joins the two halves of the jacket together.

The oil which fills the jacket is sufficiently viscous to inhibit convection currents (see Appendix A). Therefore, both jacket and fluid contribute to the thermal insulation. Sinusoidal temperature fluctuations incident on the outside of the jacket propagate inward by diffusion. The e-folding distance for a plane wave of temperature in a uniform medium is $\sqrt{\kappa/\pi f}$ where f is the frequency of the thermal signal and κ is the thermal diffusivity of the insulation. For acrylic plastics and 500 centistokes silicone oil, the diffusivities are, respectively, 1.4×10^{-3} and 1.1×10^{-3} cm^2 s^{-1}. Using the larger of these values we find the e-folding distance to be

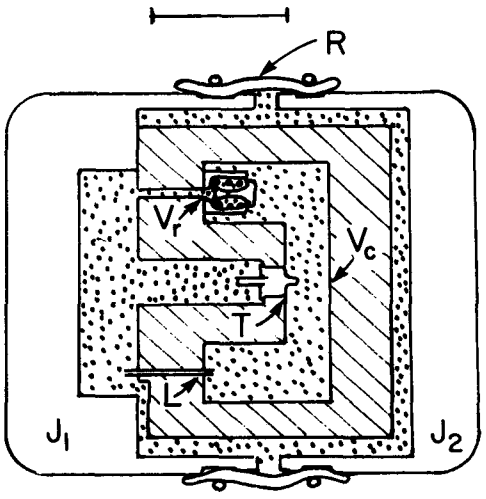

FIG. 4. Construction of the differential pressure gauge. The symbols are repeated from Fig. 2a. J_1 and J_2 are two parts of an acrylic plastic jacket that provides mechanical and thermal insulation. They are held together by the flexible rubber band R. Their relative motion, and motion of the rubber, admits ocean pressure to the interior of the gauge. V_r is one of the two over-pressure relief valves. The aluminum wall of the reference chamber V_c is cross-hatched and the silicone oil is stippled. The differential transducer T is located at the center of volume of the reference chamber. L is the capillary leak. The scale bar is 50 mm in length.

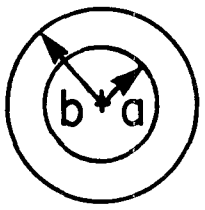

FIG. 5. Geometry of a spherical reference chamber.

f (Hz):	0.03	0.3	3.0
$(\kappa/\pi f)^{1/2}$ (cm):	0.122	0.038	0.012

In the design described below the minimum thickness of insulation is 1.27 cm. Hence, the thermal signal is attenuated by about $\exp(-10.4) = 3 \times 10^{-5}$ at 0.03 Hz. Although lower frequency thermal effects are not attenuated so severely, the background ocean pressure spectrum on the seafloor rises so rapidly that we believe thermal interference with pressure measurements does not occur for frequencies above 0.003 Hz. Ultimately, however, temperature changes will penetrate into the reference chamber and interfere with very low-frequency detection of pressures. To avoid the ensuing large spurious pressure fluctuations, we have introduced a slow leak, which vents the reference chamber with a time constant of ~ one minute.

Another possible interference signal can be generated by accelerating or tilting the pressure gauge. Either process introduces anomalous pressure gradients within both the reference chamber and the oil filling the jacket. The effects of both can be annulled by 1) placing the pressure transducer at the center of gravity of the fluid in the reference chamber and 2) making the rubber band that admits pressure to the gauge in the form of a short cylinder centered on the pressure transducer (see Appendix B). Both of these features are included in the design shown in Fig. 4, although they may not be necessary in an instrument designed for the deep seafloor because the seabed is normally mechanically quiet.

6. Protection from over-stress

The capillary leak prevents large changes of pressure difference between the reference chamber and the ocean only if pressure and temperature changes are slow. When the pressure gauge is launched from a ship at sea, these conditions may not be met and the pressure transducer might be destroyed. We attach two pressure relief valves to the reference pressure chamber for protection (Fig. 4). When the pressure difference exceeds the rating of the pressure transducer, one or the other valve opens (depending on the sign of the pressure difference). After the pressure difference drops below the rated value, the valve closes again. Under normal seafloor conditions the valves stay

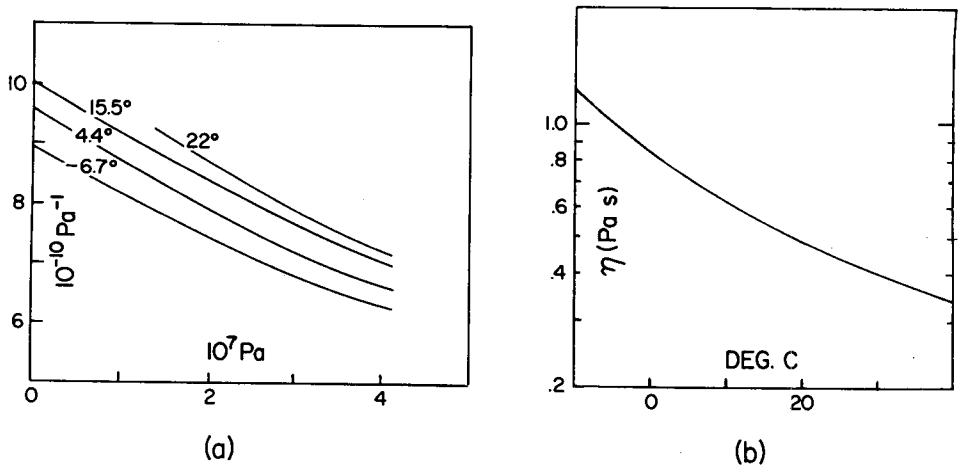

FIG. 6. (a) The adiabatic compressibility of 10 cS silicone oil as a function of pressure and temperature. Data are derived from measurements by Bornong and Hong (1977). (b) The temperature dependence of viscosity of 500 cS silicone oil at 1 atm. pressure (data from Dow Corning, the manufacturer).

closed and are sealed with o-rings and close fitting, metal-to-metal closures, which appear neither to leak appreciably nor contribute to the compliance of the chamber (Circle Seal, undated. Catalogue item 559B-1M05, Anaheim, CA.).

7. Mechanical construction and size of reference chamber

The efficiency of transfer of ocean pressures into differential pressures is given by Eq. (16), which shows that the compliance of the chamber wall and its fittings must not be large compared to the compliance of the fluid in the chamber. The fittings include "o-ring" closures, pressure relief valves and the pressure transducer. The compliance of the chamber wall can be made small by a thick wall, but the compliance of the transducer is established by its manufacture and cannot be changed. Therefore the efficiency must be controlled by choice of the fluid compliance, i.e., the compressibility of the fluid times its volume. This relationship establishes the size of the reference chamber and of the pressure gauge as a whole.

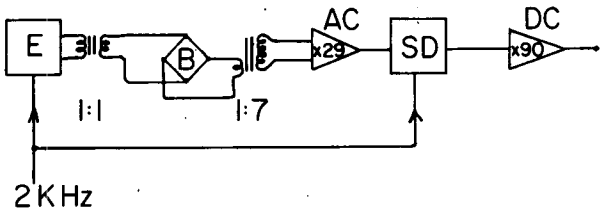

FIG. 7. Schematic diagram of circuit for the transducer. E is the sinusoidal waveform generator that excites the bridge B through an isolation transformer. The output of the bridge goes through a step-up transformer and an AC amplifier before synchronous detection (SD) and a final stage of DC amplification.

For a spherical chamber without fittings (Fig. 5), the compressibility terms that enter Eq. (16) are (Sokolnikoff, 1956)

$$k_1 = \frac{3}{E}\left[\frac{3b^3}{2(b^3 - a^3)}(1 - \nu)\right],$$

$$k_2 = \frac{3}{E}\left[\frac{b^3 + 2a^3}{2(b^3 - a^3)}(1 - \nu) + \nu\right],$$

$$k_b = \frac{3}{E}(1 - 2\nu), \quad k_d = \frac{3}{E}\left[\frac{2b^3 + a^3}{2(b^3 - a^3)}(1 - \nu) + \frac{\nu}{2}\right],$$

where E is Young's modulus for the wall material and ν Poisson's ratio. We use aluminum, a suitable material of ready availability and low mass. Its properties and the compressibility coefficients of a spherical reference chamber with outer to inner radii in the ratio $b/a = 1.2$ are:

$$E = 6.80 \times 10^{10} \text{ Pa},$$

$$\nu = 0.30,$$

$$k_1 = 1.10 \times 10^{-10} \text{ Pa}^{-1}$$

$$k_2 = 0.92 \times 10^{-10} \text{ Pa}^{-1},$$

$$k_b = 0.18 \times 10^{-10} \text{ Pa}^{-1},$$

$$k_d = 1.01 \times 10^{-10} \text{ Pa}^{-1}.$$

TABLE 2. Stations where pressure observations have been made.

Date (1983)	N Latitude	W Longitude	Depth (m)
1–3 Feb	32°18′	118°42′	1646
23–27 July	32°18′	120°44′	3847

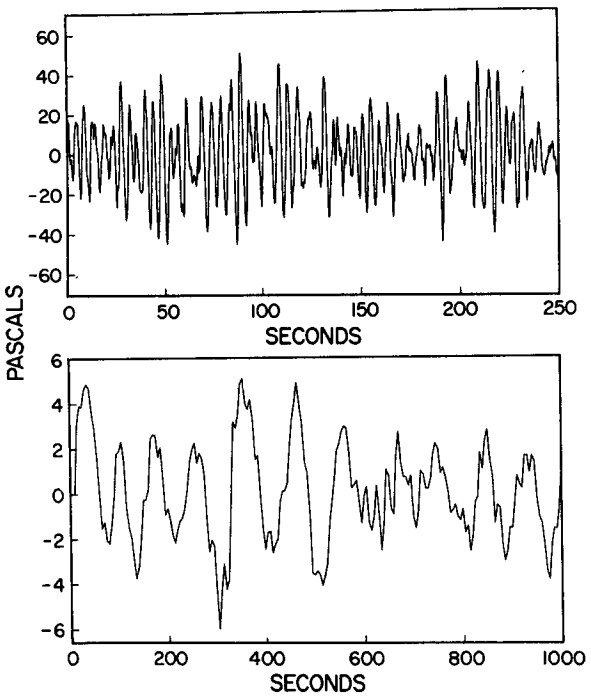

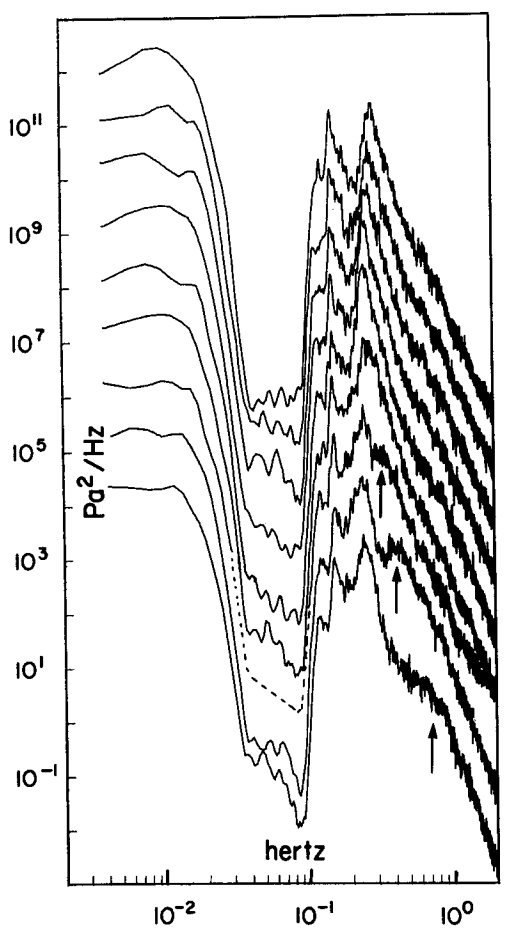

The actual value of the differential compressibility is reduced by the compliance of the transducer, seals and relief valves. We have estimated the transducer compliance from the computed motion of the diaphragm: it is only 3×10^{-17} m^3 Pa^{-1}. The compliance of the seals and values is poorly known but appears to have had a negligible influence on the measured time constant and efficiency $\tau_2/(\tau_1 + \tau_2)$ of the gauge. This remark is valid when the chamber volume is 0.31 liters.

It is impractical to construct a spherical reference chamber. In our design (Fig. 4) we have made the walls of our chosen shape sufficiently thick to make it more rigid than a sphere with $b/a = 1.2$.

8. Properties of a compressible fluid and the capillary leak

Silicone fluids provide high compressibility, a choice of high viscosities and are relatively insensitive to temperature changes. We use silicone oil with room temperature viscosity of 500 centistokes (cS) for the compressible fluid in the reference chamber. We do not know its properties at the pressure of the deep seafloor, but the adiabatic compressibility of 10 cS silicone oil has been reported by Bornong and Hong (1977), Fig. 6. According to the manufacturer, the compressibility of 500 cS oil is about 8% lower than 10 cS oil at 25°C. We have no information on the changes of viscosity with pressure, but it is unlikely to be much different proportionately from the changes of compressibility shown in Fig. 6. Accordingly, the time constant of the system

$$\tau_1 + \tau_2 = \eta V_c L(k_f + k_2)/(Qr^4)$$

is uncertain of seafloor pressures but probably not by a factor larger than 2.

We use hypodermic needle tubing for the capillary leak. The inside diameter of the tubing is 0.28 mm and the length is 37 mm. This provides a time constant of 43 s at the seafloor if the viscosity is 0.8 Pa s and the chamber volume is 0.31 liters.

9. Electrical excitation and amplification

A schematic diagram (Fig. 7) shows the signal detection system used with the pressure transducer. The silicon diaphragm bridge B is excited by a

FIG. 8. (a) Upper panel: An example of the pressure signal recorded in July 1983. Lower panel: The pressure signal after low-pass filtering to remove the microseismic signals above 0.10 Hz. (b) Sequential spectra of pressure recorded on 1–2 February 1983. Each plotted spectrum is derived from 1.14 hours of data and is displaced upwards by a factor of 10 from the previous one, for clarity. Note the spectral peak that first appears at 0.7 Hz and then decreases in frequency and increases in intensity. This peak is associated with the passage of a meteorological front over the station.

constant amplitude sinusoidal current applied to the primary of an isolation transformer. The alternating bridge output voltage is transformed and amplified before demodulation in a synchronous detector. Finally, amplification of the DC output of the detector provides an overall voltage gain of 1.8×10^4. The sensitivity expressed in terms of output voltage is 22 mV Pa^{-1}. Noise in the excitation circuit will degrade the system noise level if the bridge is out of balance. Accordingly, the bridge is carefully balanced at operating temperature before use. In fact, the bridge is rather insensitive to temperature, but we do not know the sensitivity of the balance to the high pressure of the seafloor.

10. Observations of pressure fluctuations on the deep seafloor

We have collected data at two seafloor stations (Table 2) with two versions of the gauge. An example of the pressure fluctuations is shown in Fig. 8, together with a series of frequency spectra. The dominant signal is in the frequency band of 0.11 to 2 Hz, where pressure oscillations generated by the nonlinear interaction of oppositely directed beams of sea surface wind waves are known to be transmitted to the seafloor where they generate microseismic disturbances in the seabed (Longuet-Higgins, 1950; Hasselmann, 1963). The details of the spectra in this band fluctuate in response to changing sea surface wind waves as shown by successive spectra made in February 1983 (Fig. 8).

Below the microseismic peak, the spectra drop precipitously to a level below 0.1 Pa^2 Hz^{-1} from which they rise again only at very low frequencies where long surface gravity waves no longer suffer from the severe hydrodynamic filtering of the deep water. The pressure signals of these low-frequency waves can only be brought clearly into view by low-pass filtering to remove the microseisms (as shown in Fig. 8). The spectral intensity of these waves is in quantitative agreement with the high-frequency end of the spectra measured by Filloux (1980, 1983) at two different deep water sites in the Northeastern Pacific.

11. Conclusions

The differential pressure gauge described here has been useful to measure fluctuations of pressure at the seabed with frequencies in the range extending from a few millihertz to a few hertz. Because of its low noise, the gauge is able to identify a sharp drop in the oceanic background pressure spectrum just below the microseismic peak and to delineate the changing structure of the microseismic pressures. As described herein, the gauge has a poorly defined lower frequency limit of usefulness brought about by the influence of temperature fluctuations on the oil-filled pressure reference. This limiting frequency can be lowered by increasing the thermal insulation of the reference chamber.

The gauge may have utility as a seismic detector for Rayleigh waves and *P* and *Sv* pulses. These seismic disturbances produce pressure disturbances on the seafloor and therefore should be detectable by pressure gauges. The very low oceanic background noise in the 0.03–0.1 Hz band will permit detection of these waves even when they are weak.

Acknowledgments. D. Agnew and R. Dombroski kindly called our attention to the compressibility measurements shown in Fig. 6. We are grateful for the expert help of Capt. Beattie of the research vessel *E.B. Scripps* and to the crew of this vessel. This research was supported by the Office of Naval Research.

APPENDIX A

Convective Heat Flux in the Oil-Filled Jacket of the Reference Chamber

We model the jacket by an annulus between two infinitely long, horizontal coaxial cylinders filled with a uniform viscous fluid. For positive radial temperature gradient, the fluid flow will consist of radial inward flow at the bottom of the annulus, tangential motion along the sides of the cylinder and radial outward flow at the top (Fig. A1).

The importance of unsteady temperatures is defined by $(\Delta R)^2/(\kappa\tau)$ where τ is the time scale of the temperature fluctuations at the outside of the fluid jacket and $\kappa = 0.11$ mm^2 s^{-1} is the thermal diffusivity of the oil. In our design, the radial thickness of the annulus is $\Delta R = 7$ mm. Therefore, convection can be considered steady when the time scales are long compared to 6 min. Since steady flow will produce maximum convection, we consider only this case.

In the Boussinesq approximation the density variations generate buoyancy forces but are otherwise neglected. As a consequence, we can represent the flow by a streamfunction $\psi(r, \theta)$. The boundary streamline at $r = R \pm \Delta R/2$ we take to be $\psi = 0$. This condition together with the condition for no slip, $\partial\psi/\partial r = 0$, at the same boundaries constitutes the essential conditions of the problem. Owing to the great viscosity of the oil in the jacket, the Rayleigh number

$$A = \alpha g \Delta T (\Delta R)^3/(\kappa\nu) \qquad \text{(A1)}$$

is rather small, about 30 for $\Delta T = 10$ K. (The symbols are α, thermal expansion coefficient; g, acceleration of gravity; $\Delta T/\Delta R$, radial temperature gradient; κ and ν, thermal diffusivity and kinematic viscosity, respectively.) Therefore, the temperature distribution will differ only slightly from that of a nonconvecting material, and may be considered to form a uniform gradient ($\Delta T/\Delta R \sim \partial T/\partial r$ since $\Delta R/R \ll 1$). Furthermore, the nonlinear terms in the

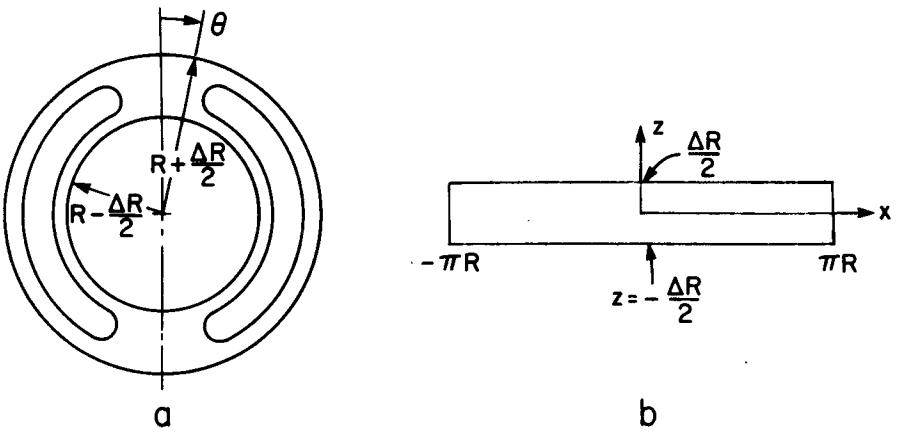

FIG. A1. Convection in an annulus formed between two cylinders. Cross section (a) shows streamlines. Diagram (b) shows flattened geometry.

equations of motion will be small. The equation governing the streamfunction [modified from Eq. (3.2) of Gill, 1966] is

$$\nabla^4\psi = -A\kappa(\Delta R)^{-4}\sin\theta. \tag{A2}$$

For simplicity we use the flattened geometry, shown in Fig. A1, in which rectangular coordinates replace polar according to

$$x = r\theta; \quad z = r - R.$$

Equation (A2) becomes

$$\nabla^4\psi = -A\kappa(\Delta R)^{-4}\sin(x/R), \tag{A3}$$

with boundary conditions ψ, $\partial\psi/\partial x$ both vanishing for all x on $z = \pm\Delta R/2$. An approximate form that satisfies the boundary conditions is

$$\psi = f(z)\sin(x/R), \tag{A4}$$

where

$$f(z) = a[1 - 2z^2(\Delta R/2)^{-2} + z^4(\Delta R/2)^{-4}].$$

With this form

$$\nabla^4\psi = \{f'''' - 2R^{-2}f'' + R^{-4}f\}\sin(x/R), \tag{A5}$$

where primes denote differentiation. Because of the smallness of $(\Delta R/R)^2$ we neglect all but the first term in the braces. This leads to

$$a = -A\kappa/384. \tag{A6}$$

The maximum radial velocity occurs at $(r, \theta) = (R, \pi)$ where it is

$$w = (\partial\psi/\partial x)_{\max} = A\kappa/(384R).$$

The convected and conducted heat fluxes are of order

$$\rho_f c_p w\Delta T \quad \text{and} \quad \rho_f c_p \kappa\Delta T/\Delta R,$$

respectively. The ratio of the convected to conducted flux is

$$(A/384)(\Delta R/R);$$

therefore, the convected flux is quite negligible in ordinary circumstances.

APPENDIX B

The Pressure Distribution in an Accelerated or Tilted Gauge

Consider the pressure gauge illustrated in Fig. (2). When it is tilted or accelerated, the pressure gradient within the reference chamber is changed and the pressure at the position of the transducer may alter.

Let the volume, mass, density and pressure of the fluid within the reference chambers be V, m, ρ, and p, respectively. The relations between them are

$$m = \int_V \rho dV, \tag{B1}$$

$$\rho = \rho_0(1 + kp), \tag{B2}$$

and according to the hydrostatic relation

$$\frac{dp}{dz} = -a\rho, \tag{B3}$$

provided we regard a as the effective combination of the acceleration of gravity and the imposed acceleration, while the axis of z is directed appropriately. The integral of (B3) is

$$1 + kp = c\exp(-a\rho_0 kz),$$

or to a sufficient approximation,

$$1 + kp = c(1 - \beta z), \tag{B4}$$

where $\beta = a\rho_0 k$ and c is an unknown constant. By combining (B1) and (B4) we find

$$m = \rho_0 \int_V A(z)c(1 - \beta z)dz,$$

where $A(z)$ is the area of the reference chamber in sections taken at right angles to the z axis. Thus,

$$m = \rho_0 Vc(1 - \beta\bar{z}),$$

where

$$\bar{z} = \frac{1}{V}\int A(z)zdz \qquad \text{(B5)}$$

is the z coordinate of the center of volume of the chamber. We now move the origin of coordinates to the center of volume so that $\bar{x} = \bar{y} = \bar{z} = 0$. Then (B5) shows that

$$c = \frac{m}{\rho_0 V} \qquad \text{(B6)}$$

is a constant independent of the acceleration and the direction of acceleration. From (B6) and (B4) one finds the pressure in the chamber

$$p = -\frac{1}{k} + \frac{m}{\rho_0 Vk} - \frac{m}{V}az.$$

Hence, at the center of volume the pressure depends on only the mass of fluid within the reference chamber, not the acceleration.

In addition to the effects of acceleration on the fluid, we must also expect an acceleration effect on the diaphragm of the transducer. A first-order correction could be made by placement of the transducer at a slight distance from the center of volume; in our case such a refinement is unnecessary because the mass per unit area of the diaphragm (63 g m^{-2}) is negligible in comparison with the mass per unit area of the fluid that it faces (~20 kg m^{-2}).

Finally, we may consider the effect of accelerations on pressure in the oil outside the reference chamber. Consider the rubber band which admits ocean pressure to the gauge. The pressure at the center of this band will approximate closely the ocean pressure, regardless of accelerations. Hence, by centering the band on the transducer, the acceleration effect is minimized.

REFERENCES

Bornong, B. J., and V. T. S. Hong, 1977: Investigation of compressible fluids for use in soft recoil mechanisms. Report ASD IR 3-77, U.S. Army LCWSL, ARRADCOM, Dover, NJ.

Filloux, J. H., 1980: Pressure fluctuations on the ocean floor over a broad frequency range: New program and early results. *J. Phys. Oceanogr.*, **10,** 1959–1971.

——, 1983: Pressure fluctuations on the ocean floor off the Gulf of California: Tides, earthquakes, tsunamis. *J. Phys. Oceanogr.*, **13,** 783–796.

Gill, A. E., 1966: The boundary layer regime for convection in a rectangular cavity. *J. Fluid Mech.*, **26,** 515–536.

Hasselmann, K. A., 1963: A statistical analysis of the generation of microseisms. *Rev. Geophys. Space Phys.*, **1,** 177.

Longuet-Higgins, M. S., 1950: A theory of the origin of microseism. 1. *Phil. Trans. Roy. Soc. London,* **A243,** 1–35.

Nichols, R. H., 1981: Infrasonic ambient ocean noise measurements: Eleuthera. *J. Acoust. Soc. Amer.*, **69,** 974–981.

Perrone, A. J., 1969: Deep-ocean ambient-noise spectra in the Northwest Atlantic. *JASA,* **46,** 762–770.

Sokolnikoff, I. S., 1956: *Mathematical Theory of Elasticity,* 2nd ed., McGraw-Hill, 343 pp.